7518-8-F

AD 646243

BASIC STRUCTURE OF INFRARED GLASSES

Final Report

1 August 1965 Through 31 December 1966

W. C. LEVENGOOD
T. S. VONG

January 1967

INFRARED AND OPTICAL SENSOR LABORATORY
Willow Run Laboratories
THE INSTITUTE OF SCIENCE AND TECHNOLOGY

Distribution of this document is unlimited.

Contract Nonr- 224(57)

ARCHIVE COPY

DDC
RECEIVED
FEB 6 1967
C

AD

AD 646196

AMRA CR 66-05/7

AMRA CR 66-05/7

CENTER FOR HIGH ENERGY FORMING

SIXTH QUARTERLY REPORT

OF TECHNICAL PROGRESS

G. A. Thurston

January 1, 1967

U. S. Army Materials Research Agency
Watertown, Massachusetts 02172

Martin Company
A Division of Martin Marietta Corporation
Contract DA 19-066-AMC-266(X)
The University of Denver
Denver, Colorado

Sponsored by

Advanced Research Projects Agency

ARPA Order No. 720

FEB 6 1967

Distribution of this document is unlimited.

ARCHIVE COPY

WHITE SECTION ☑
BUFF SECTION ☐
Statement
AVAILABILITY CODES
L. and/or SPECIAL

NOTICES

Sponsorship. The work reported herein was conducted by the Willow Run Laboratories of the Institute of Science and Technology for the U. S. Navy, Office of Naval Research, under Contract Nonr-1224(57) (ARPA Order 269, Program Code No. 5730). Contracts and grants to The University of Michigan are administered through the Office of the Vice-President for Research.

Reproduction. Reproduction in whole or in part is permitted for any purpose of the United States Government.

DDC Availability. Qualified requesters may obtain copies of this document from:

Defense Documentation Center
Cameron Station
Alexandria, Virginia 22314

Final Disposition. After this document has served its purpose, it may be destroyed. Please do not return it to the Willow Run Laboratories.

7518-8-F

BASIC STRUCTURE OF INFRARED GLASSES

Final Report

1 August 1965 Through 31 December 1966

W. C. LEVENGOOD
T. S. VONG

Distribution of this document is unlimited.

January 1967

Infrared and Optical Sensor Laboratory
Willow Run Laboratories
THE INSTITUTE OF SCIENCE AND TECHNOLOGY
THE UNIVERSITY OF MICHIGAN
Ann Arbor, Michigan

PREFACE

The work reported herein was conducted at the Willow Run Laboratories of The University of Michigan's Institute of Science and Technology for the U. S. Navy, Office of Naval Research, under Contract Nonr-1224(57) (ARPA Order 269, Program Code No. 5730). Lieutenant B. Finlayson was the contract monitor.

ABSTRACT

A phenomenological theory, designated herein as the unified glass theory, is presented. The theory introduces the concept of order-disorder transitions and liquid-model transformation within a glass network and was found to be useful in elucidating and predicting structural behavior. The degree of order and the structural characteristics of a glass system were represented by three existing models of liquid structure: Bernal, Stewart, and Frenkel. The unification of these three liquid models constitutes the basis of the proposed theory. Structure-sensitive flaws were utilized extensively in the study to facilitate the formulation of this network hypothesis.

The unified glass theory has been applied successfully in categorizing various investigated vitreous systems, among them a nonoxide arsenic trisulfide glass, metaphosphate glasses, and barium silicate infrared systems. Microyield phenomena were critically examined, and the relationships between trace width and flaw number parameter are discussed. A correlation was suggested between the critical stress of defect formation and liquidus temperatures within a field of barium silicate infrared glasses.

CONTENTS

Preface iii

Abstract v

List of Figures viii

1. Introduction 1

2. Relationship Between Flaw Formation and the Unified Theory of Glass Structure 2
   - 2.1. Flaw Formation and the Unified Glass Theory 4
   - 2.2. Flaw Formation Versus Breaking Strength 4
   - 2.3. Energy of Flaw Formation 6

3. Barium Silicate Infrared Systems 8
   - 3.1. Relationship Between b Values and Critical Stress 8
   - 3.2. Indicated Relationship Between Critical Stress and Liquidus Temperature 10
   - 3.3. Comparison of Flaw Parameters and Fractional Absorption Values 12

4. Structure of Arsenic Trisulfide Glasses 13
   - 4.1. Predicted Structure of Arsenic Trisulfide 13
   - 4.2. Suggested Strength Alterations in Arsenic Trisulfide Systems 14

5. Examination of the Su and Shih Data in Relation to the Unified Theory 14
   - 5.1. Predicted Structure 14
   - 5.2. Comparison of Experimental Data with Predicted Structure 15

6. Microyield as Related to the Unified Theory of Glass Structure 16
   - 6.1. Trace Width and Flaw Length as a Measure of Microyield 16
   - 6.2. Microyield and Ionic Field Strength 18
   - 6.3. Compressibility Measurements 18

7. Application of Findings to Infrared Transmitting Materials 19
   - 7.1. Flaw Formation and Plastic Flow 19
   - 7.2. Alterations in Plastic Flow Processes 20

8. Summary and Conclusions 21

References 23

Distribution List 24

BLANK PAGE

BASIC STRUCTURE OF INFRARED GLASSES

1
INTRODUCTION

During the initial phases of our investigations of the basic structure of glasses that transmit infrared light, the general experimental approach consisted of examining variations in the internal bonding energies with the level of dopant material. Structure-sensitive surface flaws were utilized as a means of quantitatively determining these energy changes. A description of the indenter technique used to produce these flaws under controlled loading conditions, and the empirical relationships for determining the critical stress for flaw formation were presented in a previous progress report [1]. The quantitative flaw parameters were also examined in relation to variations in the infrared spectra of the glasses, and the data obtained in these initial investigations strongly suggest that the approach of relating the spectral characteristics to specific thermal and compositional alterations in the structure of the glasses provide information about variations in the internal bonding energies. Alterations in the flaw parameters and infrared transmission characteristics were found to agree with theoretical predictions of internal energy changes based on the manner in which a specific ion entered the network of the glass.

After positive results were obtained in the initial exploratory phases of this project, efforts were directed toward organizing the data and information into a unified theory of glass structure. To this end we have formulated the initial framework of a network hypothesis which in terms of related experimental support may be considered as having a phenomenological foundation. This theory agrees with the observed internal energy variations in a number of infrared vitreous systems. The applicability of this theory was checked on both infrared and noninfrared glasses.

Tentatively, the unified theory may be briefly stated as follows:

> Vitreous structures tend to transform continuously from a network characteristic of one type of liquid structure to that of a different structure, depending on the induced thermodynamic or compositional alterations.

Under this unified concept of liquid transformations, order-disorder transitions are examined, and determination of whether a given structure is more closely repre-

sented by a Bernal, Stewart, or Frenkel type of liquid model* is considered informative.

The need for this unified theory and consideration of order-disorder transformation occurs because no well-defined model can be representative of all inorganic vitreous networks: the inherent problem of encompassing all of the various transitions in liquid structure is too great and a single model would be meaningless if the details of structural alterations in many diverse systems were to be accounted for.

We realize that any theory presented in its initial form is subject to alterations and modifications; therefore this first presentation may be considered as a template or guideline for future studies.

2
RELATIONSHIP BETWEEN FLAW FORMATION AND THE UNIFIED THEORY OF GLASS STRUCTURE

Before we can approach the subject of flaw formation, we must first consider what is really meant by a glass or liquid structure.

In the discussion of liquids in reference 6, Weyl and Marboe employ three basic models to tentatively describe the atomic and molecular arrangements in vitreous systems. These models are used to predict the ease with which a given structure may form a glass by rapid cooling:

(1) Bernal "flawless liquid"—This is described as a structure approaching a perfect crystal which is essentially free of flaws. With increasing thermal energy this covalent structure gradually changes from a crystal to a liquid through decreasing binding forces in the lattice. Example: silica.

(2) Stewart "orientable liquid"—This structure contains molecular arrays showing various degrees of order and orientation. With these oriented groupings glasses may readily form when the material is supercooled. Examples: boron oxide and sulfur.

(3) Frenkel "fissured liquid"—This is the antithesis of the Bernal model, and it is assumed that the liquid is permeated with large numbers of fissures or surfaces of broken submicroscopic bonds. These fissures are conceived of as having dynamic characteristics in that they may close and form spontaneously. This category represents ionic crystals with sharply defined melting points and those structures which cannot be supercooled to the point of forming a glass. When the melting point of the crystal is reached, it is

*See section 2.3.

assumed that there is a tremendous increase in the density of these internal fissures to form the liquid phase. Example: sodium chloride.

Glasses may have molecular properties which may be represented by all three types of these liquid models but in varying degrees. In each given system, one type of model may be most characteristic of that particular liquid structure. Experimental evidence suggesting continuous changes in the liquid structure of glasses was recently demonstrated in systems with ionic substitutions [7]. These studies were utilized to form the initial framework of the unified theory of glass structure. By adding various cations to a base system, changes in the flaw parameters were shown to follow patterns governed by the field strength and manner in which a given ion entered the network. A schematic showing the changes in the flaw parameters with additions of network-modifying ions added to a base system is shown in figure 1 along with additional notations. Superimposed on this figure are indicated regions in which a particular liquid

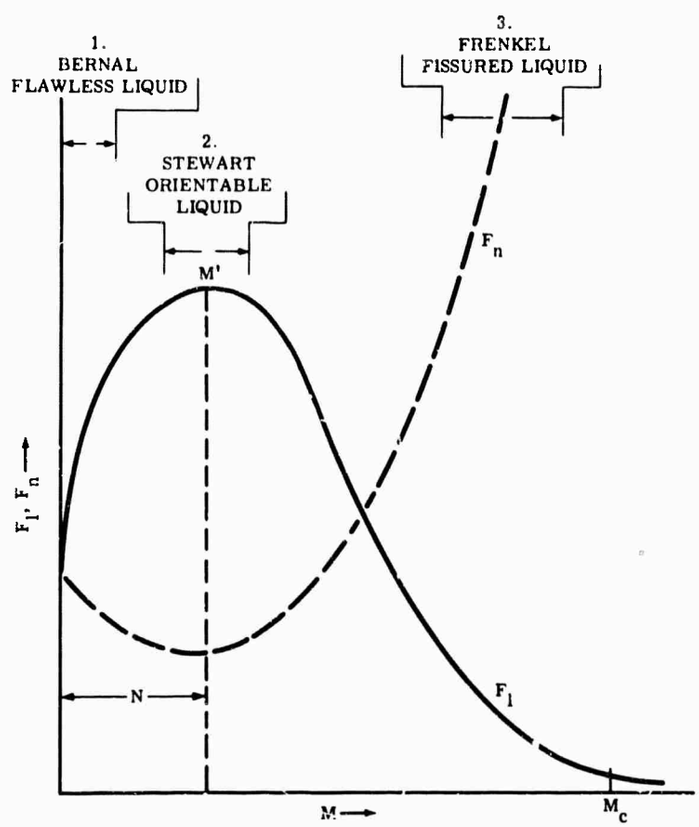

FIGURE 1. SCHEMATIC SHOWING EFFECT OF NETWORK-MODIFYING SUBSTITUTIONS ON FLAW PARAMETERS. Three liquid model regions are designated.

model is believed to be predominant. It should be pointed out, however, that before ions are substituted (left ends of curves) it is not assumed that the glass is a flawless Bernal type of structure but rather is less permeated with flaws than after a substitution has been made. In figure 1, N represents the number of cations necessary to produce the maximum, M', in the flaw-length curve. At this maximum it is assumed that the structure is now of the Stewart type, with the greatest number of orientable structures and a minimum number of internal fissures indicated by the minimum in the F_n curve. As cation additions increase, the disruption of internal bonds becomes more frequent and the number of fissures drastically increases, as shown by the rapid rise in the F_n curve. At the point designated by M_c in this figure, crystallization occurs, and just preceding this we have a structure which is permeated with fissures and is of the Frenkel type. With the substitution of ions in the network, we may therefore alter the structure and develop characteristics typical of all three models of the liquid state.

2.1. FLAW FORMATION AND THE UNIFIED GLASS THEORY

The demonstration of pronounced variation in the breaking strength as a function of changes of flaw characteristics provides intriguing questions regarding detailed variations in the structure of the various glasses studied. For example, the strength of vitreous solids (fig. 2) can be predicted from knowledge of the composition and flaw parameters.

Before we discuss details of variations in the networks of different types of glasses in relation to liquid structure, examination of the relationship between surface flaw formation and the unified theory of glass structure appears fruitful. One of the important aspects of the unified theory is the possibility of making predictions regarding the basic liquid structure and then utilizing this information as a means of increasing the inherent strength of the material without impairing the optical properties. For the many infrared glasses with very weak networks, the unified theory and knowledge concerning the liquid structure may be used to improve the strength of the glass.

The basic research that led to the conclusion that surface flaws are a direct indication of the breaking strength of the material was not conducted as a part of this project, but that part of study is reviewed below since it is pertinent to the development of the unified theory [2].

2.2. FLAW FORMATION VERSUS BREAKING STRENGTH

The general method of determining the mean breaking strength of fresh breakage surfaces produced by concentrated forces was similar to that employed by Argon, Hor., and Orowan [3]. A 1/8-in.-diameter steel ball was pressed into the fresh surface until breakage occurred. The ball was mounted on a Tinius Olsen tensile strength tester. The breakage results were expressed

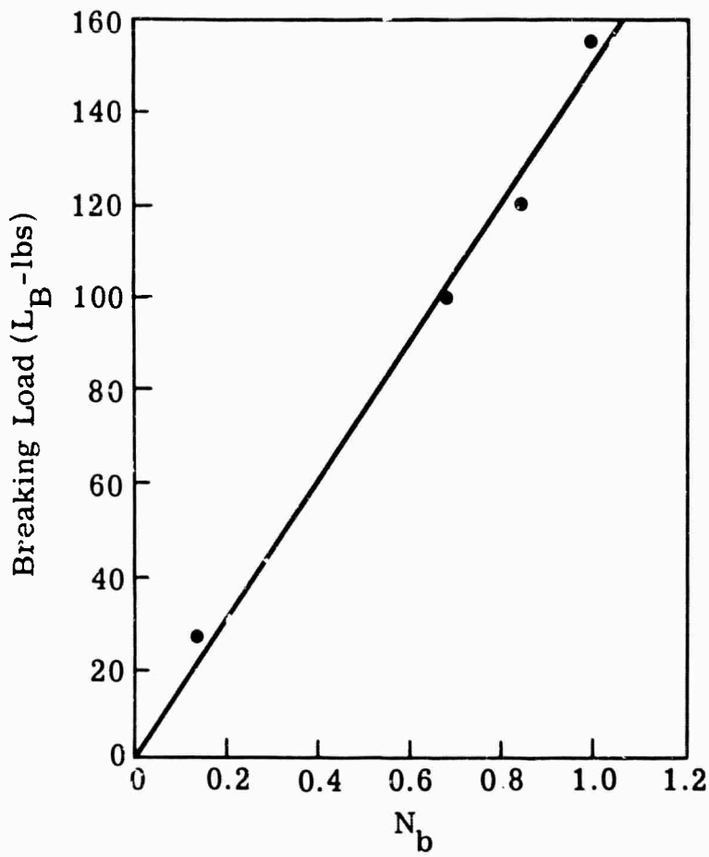

FIGURE 2. VARIATION OF BREAKING STRENGTH WITH LINEAR FLAW FORMATION IN SYNTHETIC GLASSES

as the recorded load L_b (in pounds) necessary to produce a visible Hertz cone fracture (generally a faint click could be heard when the visible crack formed). The flaw parameters were determined in the usual manner [1]. In figure 2 the agreement between the breaking load and the N_b product is shown for four synthetic glasses. (The N_b product is a measure of the total bond readjustment in a given network and is defined by

$$N_b = F_\ell F_n \tag{1}$$

where F_ℓ is the mean flaw length and F_n the flaw number on a given test surface.) The lowest point on figure 1 is the value obtained for fused silica, and the three upper points are for soda-lime-silica experimental glasses. Commercial glasses demonstrate the same linear relationship between the N_b flaw parameter and the breaking load, and the significance of this relationship may be seen by considering the role that the surface flaws play in the actual breaking process.

2.3. ENERGY OF FLAW FORMATION

To obtain some idea of the energy of flaw formation in relation to an actual breakage crack in the material, the flaws were compared with hypothetical dimensions for microcracks. Although the methods used in these calculations provide only approximate values, the order of magnitudes may be compared with the surface energy involved in the formation of a macroscopic fracture in a given vitreous network. A terminal stress σ_t occurs at the end of the flaw initiated at the trace line [1] and is given by

$$\sigma_t = KP/F_\ell^2 \tag{2}$$

where K is a constant involving Poisson's ratio ν as

$$K = (1 - 2\nu)/2\pi \tag{3}$$

If a stress σ_n is applied normal to a surface, the length C of an induced flaw or "microcrack" has been given by Cottrell [4] as

$$C = \frac{2G\gamma'}{\pi(1 - \nu)\sigma_n^2} \tag{4}$$

and in terms of the applied stress

$$\sigma_n = \left(\frac{2G\gamma'}{(1 - \nu)C}\right)^{1/2} \tag{5}$$

where G is the shear modulus (for glass 2.8×10^{11} dynes/cm^2), ν is Poisson's ratio (1/3 for glass) and γ' is the effective surface energy. This effective surface energy represents the energy involved in the flaw formation and is not the true surface energy of the material. Since C and F_ℓ are two different symbols for flaw length, the Cottrell stress in equation 5 and the terminal stress in equation 2 can be combined to give γ' in terms of the measured parameters:

$$\gamma' = \frac{(1 - \nu)K^2P^2}{2(F_\ell)^3G} \tag{6}$$

Using a load P = 500 g on the indenter produces flaws whose average length F_ℓ is around 0.07 cm. After insertion of these values in equation 6, the effective surface energy of flaw formation is determined to be

$$\gamma' \approx 11.4 \text{ ergs/cm}^2 \tag{7}$$

It is noteworthy that this value is approximately 1/30 the reported value for the surface energy involved in the creation of a fresh surface (~ 300 ergs/cm^2). The effective surface energy in-

volved in flaw formation is therefore considerably less than the surface energy necessary to produce separation or cleavage in the structure. If we assume that the effective surface energy given in equation 7 is an approximation of the actual energy of flaw formation, then we may speculate as to the involvement of the flaws in the fracture process. Since the surface energy of flaw formation is considerably less than the energy of crack development, an applied mechanical force leads first to flaw formation, thereby locally relieving the mechanical or thermally applied stress, and by this mechanism delays the formation of a macroscopic fissure.

That a continued increase in applied stress will cause a local buildup of flaws in a mechanically loaded area has been shown experimentally by Levengood [5]. The flaws may, during this buildup, combine to form a microcrack (just at the limit of visibility) leading to the final rupture of the material. Assuming an incremental increase of approximately 11 ergs/cm^2 in effective surface energy for each flaw contributing to the final microcrack, it may be seen from equation 7 that it is only necessary to combine about 30 flaws to increase the surface energy locally to the point of crack formation.

Although it has been shown that flaw buildup precedes crack formation, the actual mechanism by which the linear flaws combine to form a microcrack is not precisely understood. Since, however, the linear flaw characteristics are different in different systems, a relation between the values of breaking strengths and the flaw parameters would be expected if this concept of linear flaw involvement in fracture processes is sound. A critical test for the validity of this hypothesis of incremental effective surface energy increase was made by comparing the experimentally determined values of breaking strength with the flaw parameters in various types of glasses. Figure 2 shows experimental data for several glasses, and the linear relationship does indeed demonstrate close agreement between the flaw buildup and the breaking stress.

It is interesting to note from figure 2 that the curve extrapolates to zero strength at zero N_b product. This zero extrapolation indicates that, if we have a hypothetical glass with zero N_b, the structure would be completely brittle or rigid and could not locally relieve stress by flaw formation. Such a structure would, therefore, not support a localized force without fracture. The fact that the point for fused silica in figure 2 (lowest point on curve) disclosed a very low strength as well as low N_b under the localized concentrated force indicates a brittle structure. Although fused silica fibers are known to be very strong under uniform tensile stresses, the situation is considerably different when the forces are localized and shear stresses are created. Under conditions of nonuniform loading, the very rigid Si-O network does not yield; and this results in gross or complete bond breakage at low applied stresses.

From these well-defined alterations in structure, induced by the modifying cations, we may now proceed to examine various infrared systems using the three liquid models.

The question which now presents itself is whether one can extrapolate to other compositions and other types of glass networks.

3
BARIUM SILICATE INFRARED SYSTEMS

The glasses in this group represent those studied by Cleek at the National Bureau of Standards and contain oxide substitutions for silica. The flaw parameters in these glasses were studied systematically, and the results might be summarized by saying that the nature of the flaw characteristics indicates that these systems are of the Frenkel type. The structures display a low value of F_ℓ and a high F_n which, as may be seen in figure 1, is represented by the right end of the curve and approaches the crystalline state. In terms of the unified theory, a network representing this Frenkel region is thought of as possessing discrete regions of high order imbedded in a matrix of lesser order. The heterogeneity of this type of structure would account for the nucleation of a large number of flaws because one would expect weak regions at the boundary between the high-order areas and the matrix with the lesser degree of order. This heterogeneous type of model determines the Frenkel or fissured type of liquid system as represented by the barium silicate glasses.

In two different barium silicate systems, one containing zinc oxide substitutions and the second titanium dioxide substitutions, the flaw-length values were plotted as a function of the square root of applied load to obtain the value of critical stress (see ref. [1] for details of calculation). The basic relationship between flaw length and load is

$$F_\ell = \left(\frac{K}{\sigma_c}\right)^{1/2} P^{1/2} + b \tag{8}$$

where b is a constant resulting from a threshold stress which must be introduced into a given network to initiate flaws. It has been shown that for glasses containing a high degree of order this constant is generally negative. It is not surprising therefore to find that the b values in the Frenkel type of systems represented by the barium silicates were indeed of negative value. The critical stress values were also lower in these glasses than for other systems. This also might be expected from the weak heterogeneous nature of the network in a Frenkel system.

3.1. RELATIONSHIP BETWEEN b VALUES AND CRITICAL STRESS

During the course of investigating the various infrared systems and obtaining the detailed variations in flaw length as a function of applied load, it was found that there was a relationship

between the b values representing the initial stress to initiate flaws and the critical stress of flaw formation. In general, it is believed that this intercept constant b represents a yield which in crystals might be defined as the region of "easy glide" as the initial load is applied. In an ordered system this easy glide would be fairly extensive and b would therefore show a high negative value. In a less ordered system of the Bernal or Stewart types, b would be expected to have a positive value.

When the b values are plotted as a function of the logarithm of the critical stress, the curves are linear and the position of the b values are indicative of different types of liquid models as represented by the unified theory. To demonstrate this relationship between the yield in the network and the values of critical stress for a number of different systems, figure 3 was prepared. The lower curve was plotted from data obtained on a large number of commercial systems as well as a sample of natural obsidian glass. The natural obsidian, which is known to be permeated with crystallites, has a negative b value, like most of the infrared glasses.

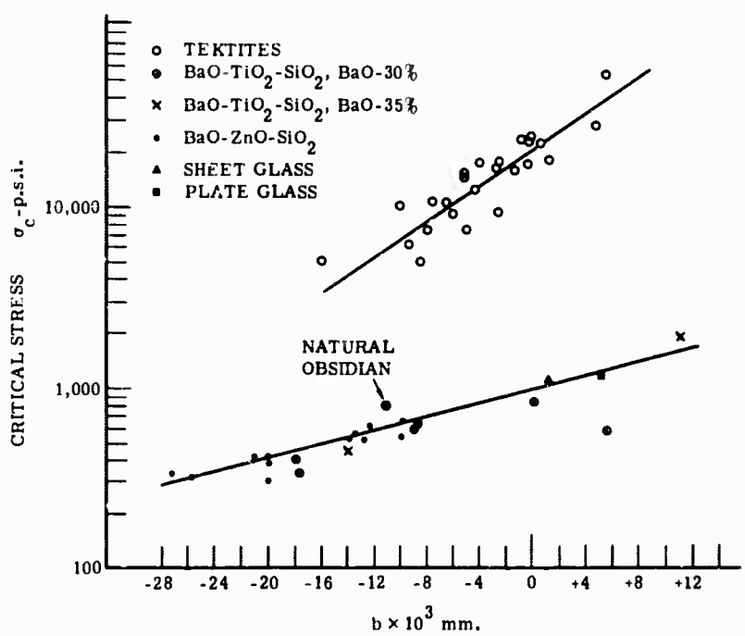

FIGURE 3. RELATIONSHIP BETWEEN b VALUES AND CRITICAL STRESS FOR VARIOUS VITREOUS NETWORKS

One infrared glass in the barium-titanium- system disclosed a pronounced positive value of b, and it was interesting to note that this particular composition was no longer in the region defined by a Frenkel fissured liquid. This glass, located in the lower curve of figure 3,

is the extreme point on the right end. Extensive flaws were observed in this glass (high F_ℓ, low value F_n), which is typical of a Stewart liquid or (region 2 in fig. 1).

The upper curve in figure 3 represents a series of unusual geologic specimens known as tektites. There are numerous theories regarding the origin of these glassy materials. One theory relates them to the melting of terrestrial materials which formed during comet or meteorite impacts on earth. Other theories suggest extraterrestrial origins such as asteroids or a lunar source. The internal elastic variations were recently examined by Levengood [8], and the nature of the variations in the flaw characteristics of these specimens suggested the formation of ordered clustered groupings in the glass network which increased with the geologic age of the tektite. The general similarities in the structure of the tektites indicated a common environmental formation, and the findings were compatible with the theory that the moon was the origin of this type of glass. As shown in figure 3, the tektites form a complete system of their own, lying on a curve of different slope than the terrestrial glasses. In most cases the b values are negative, which indicates a type of structure approaching the Frenkel fissured liquid. These findings are discussed here only to show that this method of studying internal energy and comparing the flaw parameter values is important for categorizing glasses in terms of liquid structures.

3.2. INDICATED RELATIONSHIP BETWEEN CRITICAL STRESS AND LIQUIDUS TEMPERATURE

In one series of Cleek's studies of the barium silicates with zinc oxide substituted for silica, the liquidus temperatures were reported. It was found that there was a rough correlation between the variations in the liquidus temperatures and the critical stresses (σ_c) of defect formation. This correlation becomes more pertinent when we examine the curves from the point of view of the unified theory of glass structure.

In figure 4, liquidus temperature and critical stress are plotted as functions of the zinc oxide substitution in a glass. Although the data show scatter, the critical stress appears to reach a maximum at approximately the concentration at which the liquidus temperature reaches a minimum. If a structure has a high liquidus temperature, this indicates a higher potential for crystallization (greater number of nuclei) than if it had a low liquidus temperature. The high liquidus ends of the top curve shown in figure 4 would therefore represent those structures most like a Frenkel liquid. At the minimum liquidus temperature, the structure would be more of the Stewart type. The high liquidus or fissured liquid would therefore represent weak structures, and this would explain the low values of critical stress. The low liquidus temperatures on the other hand are less heterogeneous in terms of ordered regions, and therefore σ_c increases

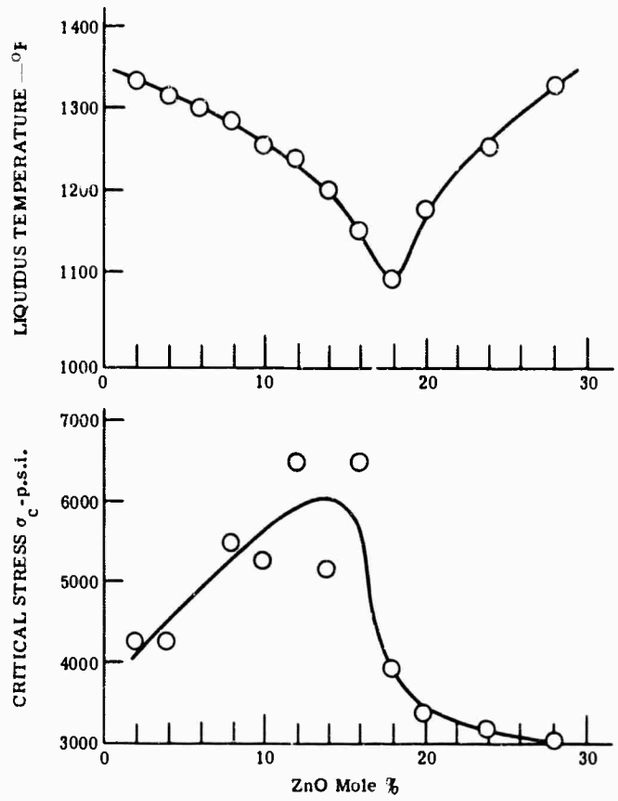

FIGURE 4. COMPARISON OF LIQUIDUS TEMPERATURES AND CRITICAL STRESS VALUES IN A BARIUM SILICATE INFRARED SYSTEM. ZnO substituted for SiO_2.

accordingly. Although the agreement between the changes in liquidus temperatures and critical stress is only roughly indicated in figure 4, this finding is important for the following reasons: first, a physical parameter related to bond strength has been shown to be related to changes in liquidus temperatures; and second, the observed changes can be explained on the basis of the unified theory of glass structure.

Table I summarizes the changes in order and the expected changes in flaw parameters in glasses with high and low liquidus temperatures. It should be kept in mind that these comparisons are qualitative only. From figure 4 and table I, it may be seen that σ_c may be used as an indication of the type of liquid structure. The changes in σ_c within a particular model may also be sensitive to variations of the liquidus temperature. It was of importance to find that σ_c may provide an indication of the type of structure since, in some systems such as the barium silicate glasses, the F_ℓ changes with composition are not pronounced nor are changes in the F_n values.

TABLE I. COMPARISON OF LIQUID MODELS WITH PREDICTED VARIATIONS IN FLAW PARAMETERS

	High Liquidus Temperature	Low Liquidus Temperature
1.	Favors Frenkel liquid	Stewart liquid
2.	Formation of discrete ordered groupings	Pseudomorphic chains
3.	Low free energy	High free energy
4.	Low σ_c	High σ_c
5.	Negative b	Positive b
6.	Heterogeneous Network	Homogeneous network

In numerous systems one must rely on the σ_c values to detect subtle variations within a given type of network; this is particularly true of the Frenkel fissured liquids.

3.3. COMPARISON OF FLAW PARAMETERS AND FRACTIONAL ABSORPTION VALUES

In all of the barium silicate systems examined, the values in the absorption bands designated α_1 and α_2 [1] were examined in relation to the compositional variation. Both the α_1 band indicating the degree of hydroxyl association in the glass and the α_2 band related to the carbonate ion disclosed complex variations with changes in the flaw parameters. The glasses previously studied showing the predicted changes in fractional absorption as a function of the flaw parameters constituted systems in which substitutions were made for network modifiers or network formers. Substitutions in the barium silicate systems were made in a more complex manner. For example, zinc oxide, which is a network modifier, was substituted for silicon dioxide, which is a network former. The previous agreement between the fractional absorption values and the flaw parameters were obtained only in systems which were either of the Bernal or Stewart type. In the Frenkel fissured liquids such as the barium silicates, the α_1 and α_2 values may depend on more complex associations between the hydroxyl or carbonate groups and the ordered groupings in the matrix. For example, hydroxyl complexes such as Si-OH-Zn may form, or the OH groups may associate with nonbridging bonds formed between the highly ordered regions and the less-ordered matrix. Such complex associations could explain the lack of correlation between flaw parameters and the fractional absorption values in the Cleek infrared systems. Because of these complex variations, the fractional absorption studies were abandoned in those glasses showing a structure such as those located in the Frenkel region (region 3 of fig. 1).

4
STRUCTURE OF ARSENIC TRISULFIDE GLASSES

During this study a successful experimental procedure was worked out for examining the flaw parameters in nonoxide arsenic trisulfide glasses. The flaw length versus applied load curve is shown in figure 5. It was gratifying to observe that the mean flaw length vs. the square root of applied load had the same linear relationship as that found in oxide glasses.

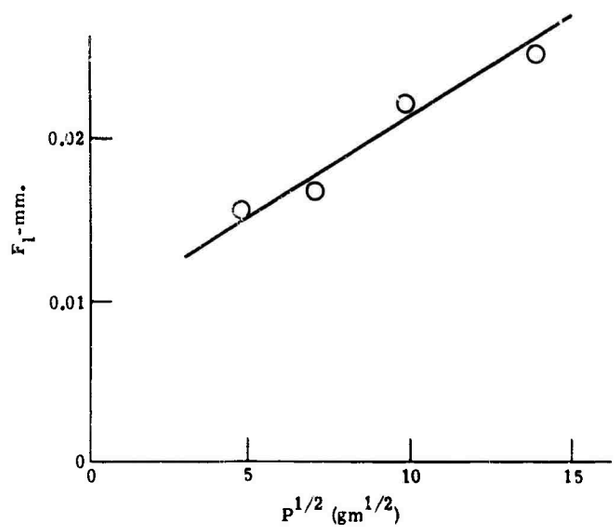

FIGURE 5. FLAW-LENGTH VARIATION WITH APPLIED LOAD ON AN ARSENIC TRISULFIDE GLASS

4.1. PREDICTED STRUCTURE OF ARSENIC TRISULFIDE GLASSES

The quantitative flaw data for this glass system are:

$\sigma_c = 5310$

$a \times 10^4 = 12$

$b = +0.009$ mm

where a = slope value.

The critical stress value is observed to be considerably higher than the values for the commercial glass systems plotted in figure 3, which is not too surprising since an arsenic trisulfide system is quite different from those of the oxide glasses. The more unexpected aspect of the quantitative flaw studies in the arsenic trisulfide system was the discovery that the slope con-

stant b had a positive value. This indicates that this nonoxide system is less characteristic of the crystalline state and is less ordered than the barium silicate infrared glasses. It has been suggested by Myers and Felty [9] and by others that the arsenic trisulfide system contains chains or long groupings of molecules, possibly pseudomorphs of S_8 ring formations. The positive b value substantiates the existence of random orientable long chain formations of a Stewart liquid. This nonoxide system contrasts with an ordered structure approaching the crystalline state, as observed in many of the other infrared glass systems.

4.2. SUGGESTED STRENGTH ALTERATIONS IN ARSENIC TRISULFIDE SYSTEMS

Because arsenic trisulfide glass lies in the region of a Stewart orientable type of liquid structure (region 2 of fig. 1), the possibility of inducing alterations in the bonding characteristics was tentatively examined. A stewart type of liquid model with orientable chains suggests that interstitials might be added which would strengthen bonds between the chains and thereby alter the strength characteristics. By adding trace amounts of impurity ions with high polarizabilities and examining the alteration in the σ_c and b values with the addition of these dopants, the mechanical properties of this material might be significantly improved without great impairment of the infrared transmission characteristics. An experimental study of this kind is being considered for future work.

5
EXAMINATION OF THE SU AND SHIH DATA IN RELATION TO THE UNIFIED THEORY

From the close correlation between predicted infrared absorption bands in metaphosphate glasses and the experimentally observed spectra, we may assume that the "zig-zag" model proposed by Su and Shih is valid [10]. This zig-zag model suggests that on the basis of the unified glass theory the structures of these metaphosphate glasses are of the Stewart type; that is, they contain long chains or groupings with weak forces between them.

5.1. PREDICTED STRUCTURE

With substitution of network formers in the Stewart region, a strong correlation has been shown between ionic field strength and the infrared absorption characteristics (see ref. [1]). In the Su and Shih work, very systematic substitutions of various network-modifying cations were made in the structure of the metaphosphate glasses and the infrared transmission was examined. From the unified theory we may advance the hypothesis, therefore, that a relationship between ionic field strength (Z/r_2) and the spectral data should be expected (Z = the charge on the ion and r = crystal radius).

5.2. COMPARISON OF EXPERIMENTAL DATA WITH PREDICTED STRUCTURE

Since in a Stewart type of model the alterations in the infrared spectra as produced by the substitution of various network-modifying ions should occur over a fairly broad spectral region, the transmission curves were graphically integrated between the 5-15 micron region. This area, expressed in arbitrary units, was plotted as a function of the field strength of the substituted cation, and the data are presented in figure 6. A decrease in the integrated area under the curve would represent increasing absorption; therefore figure 6 shows that absorption increases with increasing field strength of the substituted cation. This finding is in agreement with previous studies on glasses of the Stewart type of structure in which similar cation substitutions were made [1]. It therefore appears that the experimental data are in accord with a Stewart type of liquid composed of orientable chains. If this structure were of the Frenkel fissured type, observation of this correlation between optical absorption and the ionic field strength would not be expected.

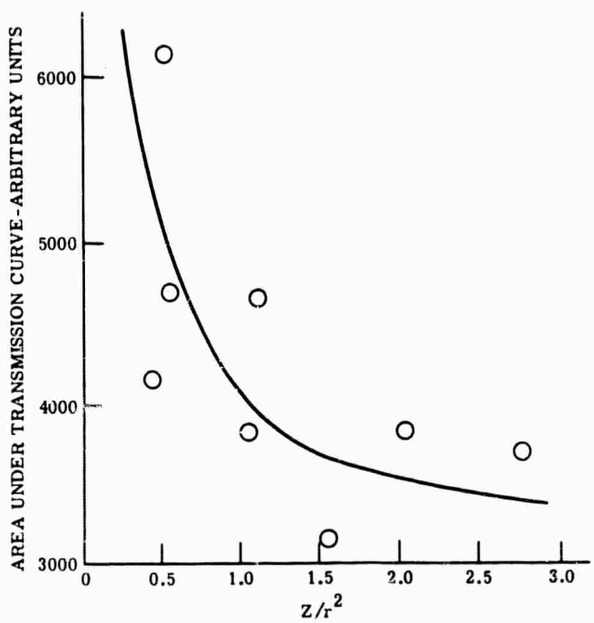

FIGURE 6. RELATIONSHIP BETWEEN INTEGRATED AREA UNDER TRANSMISSION CURVE AND IONIC FIELD STRENGTH. (From Su and Shih data.)

6
MICROYIELD AS RELATED TO THE UNIFIED THEORY OF GLASS STRUCTURE

The possibility of considering microyield or variations in the modulus of elasticity in glasses within microregions (E_{mic}) became apparent after a visit with Dr. C. J. Phillips at Rutgers University, made during this study. Phillips' empirical calculations demonstrate that there is no straightforward relationship between the macroscopically measured values of Young's modulus E and flaw length parameter F_n, which expresses the relative rigidity of the network. It had previously been suggested [7] that such a relationship might exist. Because Phillips' calculations and the flaw parameters lack correlation, we speculated that F_n might be more closely related to yield at the microscopic level rather than being related to E as measured in the "usual manner." Since the modulus of elasticity is a structure-sensitive property and might also be related to changes in the type of liquid or glass structure, we decided to examine this situation more closely.

"Usual manner" itself was considered suspect since it determines yield over macroscopic regions in the network, whereas the indenter technique applied to fresh cleavage surfaces gives yields in microscopic regions. The microyield induced by the indenter might conceivably be considerably different in magnitude from the macroscopic value of Young's modulus. It occurred to us that a parameter which we might utilize to examine microyield was the trace width (T_w) produced by the spherical dynamic indenter. Therefore, the microyield as expressed by the trace width was examined as a function of F_n.

6.1. TRACE WIDTH AND FLAW LENGTH AS A MEASURE OF MICROYIELD

If F_n is a measure of network yield (or rigidity), and if T_w might be a measure of microyield, there should be a relationship between these two parameters. Figure 7 demonstrates such a relationship between T_w and the nucleation of flaws along the trace line. These curves were obtained in soda-lime-silica systems in which univalent cations were substituted for sodium. As T_w decreases, the system would become rigid; that is, the rolling ball would penetrate less far into the surface. This increased rigidity is also reflected in a concomitant increase in the number of flaws nucleated in the system.

The increasing rigidity of the network with additions of a high-field-strength ion such as antimony are shown in figure 8 as a function of oxide concentration in the network. Here again, with a decrease in T_w, there is an increase in F_n. This same relationship has been demonstrated in many systems in which cation substitutions have been made and a pronounced change in the structure was noted.

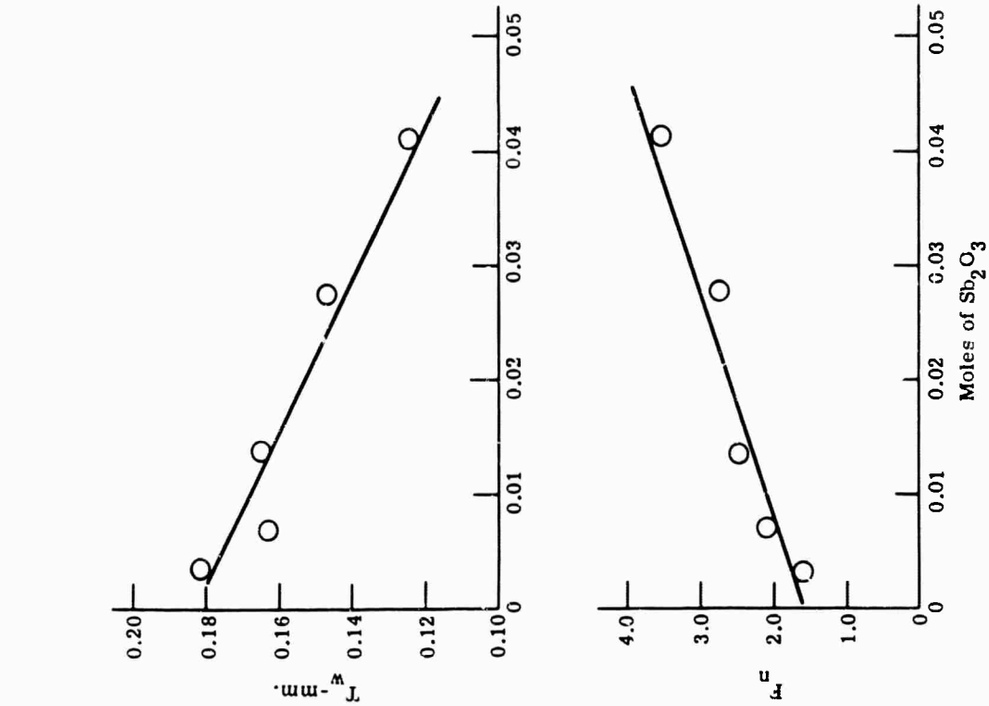

FIGURE 8. RELATIONSHIP BETWEEN FLAW NUMBER AND TRACE WIDTH WITH ANTIMONY OXIDE ADDITIONS

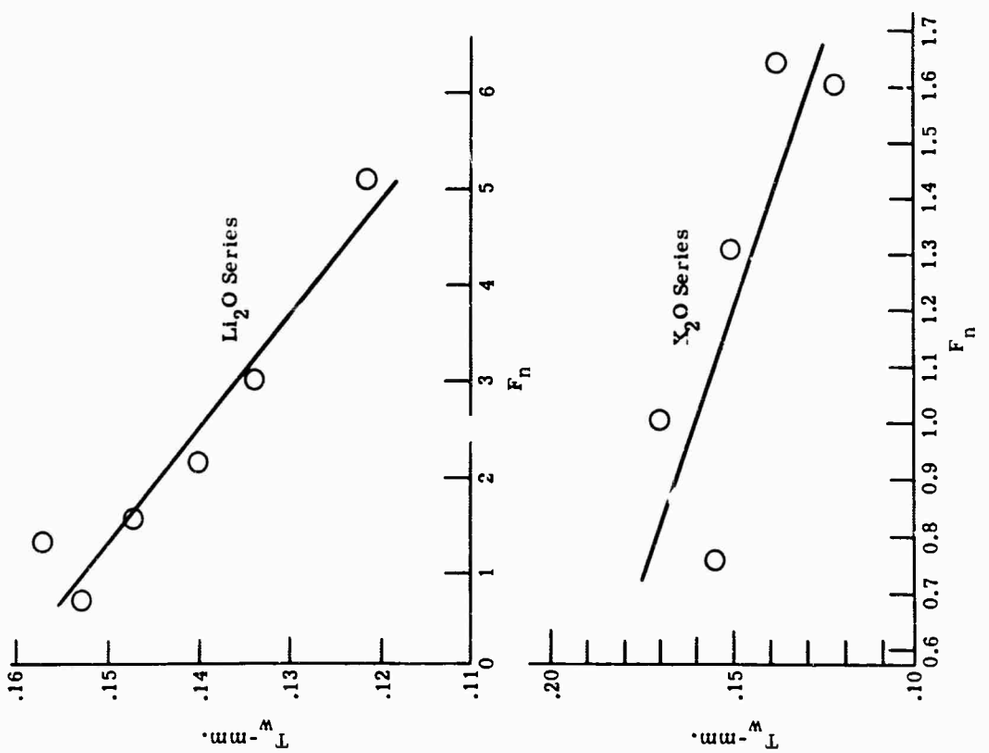

FIGURE 7. COMPARISON OF TRACE WIDTH WITH FLAW NUMBER IN TWO SODA-LIME-SILICA SYSTEMS. Li_2O and K_2O substituted for Na_2O.

6.2. MICROYIELD AND IONIC FIELD STRENGTH

To provide additional insight into the relationship between microyield and the F_n, consideration was given to the possibility that the T_w values (see figs. 7 and 8) are related to variations in the ionic configurations within the network. For ionic crystals, it has been shown [11] that the modulus of elasticity is roughly proportional to ion size as

$$E \propto Z^2/d^4 \tag{9}$$

where Z is the charge on the ion and d the distance of ion separation in the crystal. This same proportionality may be expressed in terms of ionic field strength by

$$E \propto (Z/r^2)^2 \tag{10}$$

where r is the crystal radius of the ion. From this suggested proportionality between Young's modulus and ionic field strength, it would appear advantageous in future studies to examine the microyield in various series in which systematic ionic substitutions have been made.

From these relationships and the data obtained in the preliminary studies, we can tentatively conclude that T_w is a measure of the microyield in the network and that the macroscopic value of Young's modulus cannot be relied upon to correlate with the flaw parameters. At the microscopic level, however, such correlations exist; and this demonstrates that F_n is indeed related to the microyield in the network of the glass.

6.3. COMPRESSIBILITY MEASUREMENTS

The data showing the relationship between microyield (as determined by trace width) and F_n support the contention that examining the yield in liquid structures is of great value. The manner in which a given structure readjusts under a given applied stress should depend on its inherent structure in relation to the three basic liquid models. A determination of compressibility is one way in which variations in these structures could be examined. The importance of considering the yield of glasses or the degree of compressibility has been expressed by Weyl and Marboe [6]: "From the viewpoint of the constitution of glasses it would be highly desirable to have more measurements of the compressibility of glasses whose compositions are varied systematically . . . ."

From the standpoint of a completely random network theory, the recovery rates from an initial deformation would be expected to show little or no variation. From the standpoint of distinct structures as represented by the three liquid models presented in the unified glass theory, each type of structure would, on the other hand, disclose its own characteristic elastic

recovery process. Compressibility measurements would therefore tend to corroborate or refute the unified glass theory as presented here.

Such compressibility measurements could be made on a relatively simple scale. For example, one might use a microinterferometer technique [12] and produce local deformations under compressive forces on fresh cleavage surfaces. The examination of various liquid structures by this technique is planned in future experimentation.

7
APPLICATION OF FINDINGS TO INFRARED TRANSMITTING MATERIALS

The preceding sections show that, given some glass and utilizing the parameters of surface flaw formation, we may categorize such a glass as belonging to a given type of liquid structure. The advantage of knowing in which system or type of structure the glass is located lies in being able to predict what will happen when mechanical forces are applied to the system. The state of internal order also determines how composition can be varied. Of course, much remains to be learned about subtle variations in the systems. However, if we know how the flaws interact in the glass network, we may interfere with these flaw formations and elastic energy variations with the possible outcome of enhancing the basic bond strength. Let us examine the precise relationship between the surface flaw formation and the inherent strength of the material.

7.1. FLAW FORMATION AND PLASTIC FLOW

The demonstration of a direct relationship between flaw formation and the breaking strength of various glasses (fig. 2) provides quantitative evidence for the important role that surface flaws play in bond rupture. Flaw growth apparently relieves stress in localized regions by the release of effective surface energy. The surface energy of an individual flaw amounts to about 1/30 the energy utilized in the creation of new surfaces in bond rupture. Because of their low energy, surface flaws form at critical stresses considerably below those necessary to produce fracture. In regions of locally applied forces, networks of these flaws are formed and with increasing stress may combine to form a microcrack with subsequent failure of the network.

Because of their ease of formation (at moderate stresses) and low effective surface energy, it is not difficult to conceive of these surface flaws as being involved in plastic flow mechanisms. Independent evidence for localized plastic flow in glass has been offered by D. M. Marsh [13] from experiments and a comprehensive analysis of Vickers diamond hardness tests. This author points out that brittle fracture theories are "grossly inadequate" to explain the strength behavior of glasses. Evidence of plastic flow is utilized to account for observed variations in

brittle fracture. Marsh envisions the deformation process as a uniform radial bulk flow around the point of load application.

A process of a localized plastic flow may also be accounted for at least partially by surface flaw formation. The results in the preceding sections demonstrate that, when flaw formation is extensive (large F_ℓ), the breaking force is high and the system in terms of the unified glass theory is in the Stewart region of liquid structure. The plastic flow or slip process is not a uniform radial flow around the load region but instead takes place along certain linear arrays in the network. The radial extent of these linear flaws or planes of flow is determined by such factors as applied stress surface energy as well as the type of structure or composition. A spontaneous initiation of a pattern of flaws has also been observed to take place in limited composition ranges, with the formation of interesting spiral shapes [14]. Studies of the flaw parameters indicate that this spiral pattern forms in a brittle or rigid type of network containing regions with a high degree of order. This type of structure is very definitely in the Frenkel region and contains many fissures, or is a system very near the point of crystallization. Specific groupings form localized regions of torque stress in the glass, and when one of these regions is located near or on a fracture plane, plastic flow with flaw formation which follows this torque stress field may occur. An example of this type of suggested spontaneous plastic flow in a Frenkel type of glass is shown in figure 9 within a simple soda-lime-silica system. This is just one of many qualitative effects which strongly suggest plastic flow mechanisms through flaw formation.

From the discussion above, it may be seen that both the quantitative and qualitative aspects of linear flaw formation suggest a mechanism by which vitreous structures may exhibit plastic flow. This plastic flow takes place in linear arrays at stresses considerably below the theoretical cohesive bond strength of the material.

7.2. ALTERATIONS IN PLASTIC FLOW PROCESSES

Since the results presented here demonstrate that flaw formation and basic strength are dependent on plastic flow mechanisms in a given vitreous structure, it appears worthwhile to speculate on the possible mechanisms by which the elastic yield mechanisms in glasses can be altered. Compositional variations are one obvious method which has been thoroughly discussed in the previous sections. Another more subtle technique is to add interstitial impurities. These impurities may take the form of particulate groupings in the network or interstitials such as gases which form chemical associations.

The aspect of introducing dissolved gases into the basic network of various infrared glasses has not to our knowledge been investigated to any extent. Although there is a possibility that

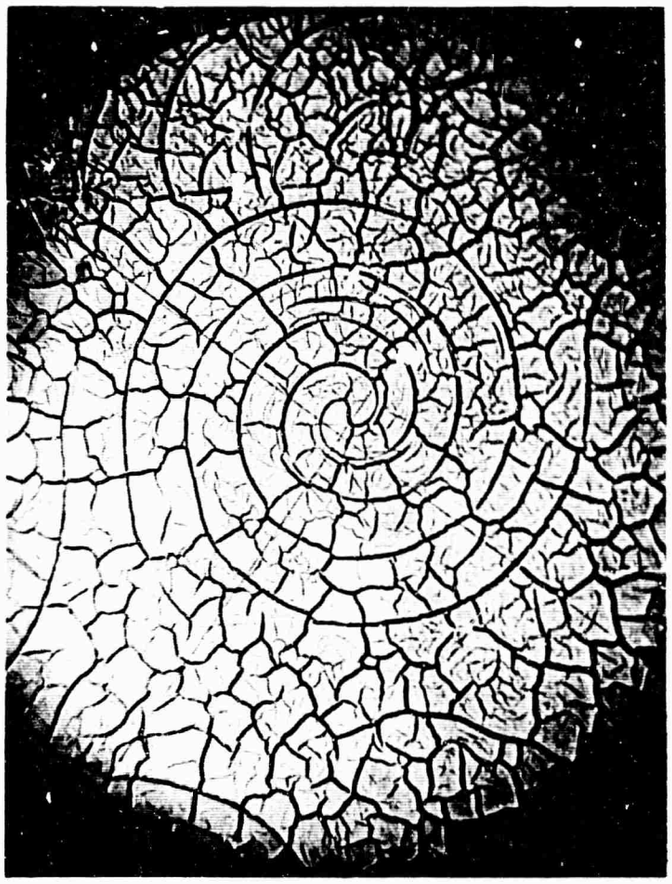

FIGURE 9. SUGGESTED SPONTANEOUS PLASTIC FLOW.
Spiral flaw pattern formed in a Frenkel-type glass.

such gases might introduce absorption bands, the increased advantage of enhancing mechanical strength might more than offset specific absorption bands introduced into the transmission spectra. The effect of these interstitial gases on flaw formation and the elastic yield properties are being considered for future studies.

8
SUMMARY AND CONCLUSIONS

The basic structure of vitreous infrared materials has been examined by utilizing structure-sensitive surface flaw formations. Variations in the internal energy of numerous glass networks as manifested by alterations in the surface flaw parameters have led to the following conclusions regarding the characterization of the basic structure of infrared vitreous materials.

(1) A unified theory of glass structure has been formulated. This phenomenological theory is based on order-disorder transitions occurring in structures which may be represented by a Bernal-flawless, a Stewart-orientable, or a Frenkel-fissured type of liquid model.

(2) In the Frenkel type of liquid structure there is no clear-cut relationship between the infrared transmission characteristics and the variations in internal order.

(3) On the basis of this unified glass theory and variations in the flaw parameters, barium silicate infrared glasses have been placed in the general category of Frenkel systems with a high degree of order.

(4) Variations in the liquidus temperature within a barium silicate infrared system have been shown to be related to the critical stress of defect formation. A high liquidus temperature favors a Frenkel-fissured liquid with low critical stress or a weak structure. A low liquidus temperature, on the other hand, favors a Stewart-orientable liquid with a higher critical stress value.

(5) An arsenic trisulfide nonoxide system was shown to possess a Stewart type of liquid structure, and this was attributed to the presence of chains, possibly S_8, in the network.

(6) From the infrared data of Su and Shih a Stewart type of liquid model was proposed for metaphosphate glasses. This was confirmed by application of the unified glass theory when network-modifying cations were introduced into the metaphosphate system.

(7) The microyield of the glass network as measured by the trace width was shown to be directly related to the flaw parameter F_n, which also is a relative measure of the rigidity of the network. This was an important finding in the sense that a trace width or microyield technique may be utilized in those systems where it is extremely difficult to find an etchant and determine the flaw parameters.

Increasing the strength in infrared materials with useful transmission characteristics may be possible. By utilizing the unified theory, the glasses may be categorized in terms of one of the three types of liquid structure. With this information alterations in the internal bond strength characteristics may be induced judiciously. Methods such as introduction of interstitial impurities including dissolved gases were suggested as possible means of altering the glass structure.

REFERENCES

1. W. L. Wolfe and W. C. Levengood, Basic Structure Glasses, Semiannual Progress Report, 1 August Through 1 February 1966, Report No. 7518-3-P, Willow Run Laboratories, Institute of Science and Technology, The University of Michigan, Ann Arbor, March 1966.
2. W. C. Levengood, "Bond Rupture Mechanisms in Vitreous Systems," J. Fracture Mech., Vol. 2, 1966, pp. 400-412.
3. A. S. Argon, Y. Hori, and E. Orowan, J. Am. Ceram. Soc., Vol. 43, 1960, pp. 86-96.
4. A. H. Cottrell, in Fracture, B. L. Averbach, et al. (eds.), Wiley, 1959.
5. W. C. Levengood, "Static Stress Fatigue and Strength of a Vitreous Silicate," J. Appl. Phys., Vol. 35, 1964, pp. 424-433.
6. W. A. Weyl and E. C. Marboe, The Constitution of Glasses, Vol. I, Wiley, 1962, pp. 128-143.
7. W. C. Levengood, "Systematics of Defect Structures in Glasses with Ionic Substitutions," J. Phys. Chem. Solids, Vol. 24, 1963, pp. 1011-1024.
8. W. C. Levengood, "Internal Elastic Energy Variations in Tektites," J. Geophys. Res., Vol. 71, 1966, pp. 613-618.
9. M. B. Myers and E. G. Felty, "The Characterization of Vitreous Inorganic Polymers by Thermal Measurements," International Conference on the Characterization of Materials, Pennsylvania State University, Nov. 16-18, 1966.
10. G. J. Su and C. K. Shih, "Infrared Spectra of Metaphosphate Glasses," Office of Naval Research, Contract No. Nonr 668(19), Dec. 1964, Univ. of Rochester Report.
11. W. A. Weyl and E. C. Marboe, The Constitution of Glasses, Vol. II, Interscience, 1964.
12. W. C. Levengood and T. S. Vong, "Observations Concerning Delayed Elastic Effects in Glass," J. Opt. Soc. Am., Vol. 49, 1959, pp. 61-66.
13. D. M. Marsh, "Plastic Flow in Glass," Proc. Roy. Soc., London A, Vol. 279, 1964, pp. 420-435.
14. W. C. Levengood, "Defect Mechanisms in a Noncrystalline Solid," J. Appl. Phys., Vol. 32, 1961, pp. 2525-2533.

BLANK PAGE

UNCLASSIFIED

Security Classification

DOCUMENT CONTROL DATA - R&D

(Security classification of title, body of abstract and indexing annotation must be entered when the overall report is classified)

1 ORIGINATING ACTIVITY (Corporate author) Willow Run Laboratories of the Institute of Science and Technology, The University of Michigan, Ann Arbor	2a REPORT SECURITY CLASSIFICATION Unclassified 2b GROUP

3 REPORT TITLE

BASIC STRUCTURE OF INFRARED GLASSES

4 DESCRIPTIVE NOTES (Type of report and inclusive dates)

Final Report, 1 August 1965 Through 31 December 1966

5 AUTHOR(S) (Last name, first name, initial)

Levengood, W. C.; Vong, T. S.

6 REPORT DATE January 1967	7a TOTAL NO OF PAGES viii + 25	7b NO OF REFS 14
8a CONTRACT OR GRANT NO Nonr-1224(57) b PROJECT NO c d	9a ORIGINATOR'S REPORT NUMBER(S) 7518-8-F 9b OTHER REPORT NO(S) (Any other numbers that may be assigned this report)	

10 AVAILABILITY/LIMITATION NOTICES

Distribution of this document is unlimited.

11 SUPPLEMENTARY NOTES	12 SPONSORING MILITARY ACTIVITY Office of Naval Research, Washington, D. C.; Advanced Research Projects Agency, Department of Defense, Washington, D. C.

13 ABSTRACT

A phenomenological theory, designated herein as the unified glass theory, is presented. The theory introduces the concept of order-disorder transitions and liquid-model transformation within a glass network and was found to be useful in elucidating and predicting structural behavior. The degree of order and the structural characteristics of a glass system were represented by three existing models of liquid structure: Bernal, Stewart, and Frenkel. The unification of these three liquid models constitutes the basis of the proposed theory. Structure-sensitive flaws were utilized extensively in the study to facilitate the formulation of this network hypothesis.

The unified glass theory has been applied successfully in categorizing various investigated vitreous systems, among them a nonoxide arsenic trisulfide glass, metaphosphate glasses, and barium silicate infrared systems. Microyield phenomena were critically examined, and the relationships between trace width and flaw number parameter are discussed. A correlation was suggested between the critical stress of defect formation and liquidus temperatures within a field of barium silicate infrared glasses.

DD FORM 1 JAN 64 1473

UNCLASSIFIED

Security Classification

14 KEY WORDS	LINK A ROLE	LINK A WT	LINK B ROLE	LINK B WT	LINK C ROLE	LINK C WT
Glasses Vitreous structures Infrared absorption						

INSTRUCTIONS

1. ORIGINATING ACTIVITY: Enter the name and address of the contractor, subcontractor, grantee, Department of Defense activity or other organization *(corporate author)* issuing the report.

2*a*. REPORT SECURITY CLASSIFICATION: Enter the overall security classification of the report. Indicate whether "Restricted Data" is included. Marking is to be in accordance with appropriate security regulations.

2*b*. GROUP: Automatic downgrading is specified in DoD Directive 5200.10 and Armed Forces Industrial Manual. Enter the group number. Also, when applicable, show that optional markings have been used for Group 3 and Group 4 as authorized.

3. REPORT TITLE: Enter the complete report title in all capital letters. Titles in all cases should be unclassified. If a meaningful title cannot be selected without classification, show title classification in all capitals in parenthesis immediately following the title.

4. DESCRIPTIVE NOTES: If appropriate, enter the type of report, e.g., interim, progress, summary, annual, or final. Give the inclusive dates when a specific reporting period is covered.

5. AUTHOR(S): Enter the name(s) of author(s) as shown on or in the report. Enter last name, first name, middle initial. If military, show rank and branch of service. The name of the principal author is an absolute minimum requirement.

6. REPORT DATE: Enter the date of the report as day, month, year; or month, year. If more than one date appears on the report, use date of publication.

7*a*. TOTAL NUMBER OF PAGES: The total page count should follow normal pagination procedures, i.e., enter the number of pages containing information.

7*b*. NUMBER OF REFERENCES: Enter the total number of references cited in the report.

8*a*. CONTRACT OR GRANT NUMBER: If appropriate, enter the applicable number of the contract or grant under which the report was written.

8*b*, 8*c*, & 8*d*. PROJECT NUMBER: Enter the appropriate military department identification, such as project number, subproject number, system numbers, task number, etc.

9*a*. ORIGINATOR'S REPORT NUMBER(S): Enter the official report number by which the document will be identified and controlled by the originating activity. This number must be unique to this report.

9*b*. OTHER REPORT NUMBER(S): If the report has been assigned any other report numbers *(either by the originator or by the sponsor)*, also enter this number(s).

10. AVAILABILITY/LIMITATION NOTICES: Enter any limitations on further dissemination of the report, other than those imposed by security classification, using standard statements such as:

(1) "Qualified requesters may obtain copies of this report from DDC."

(2) "Foreign announcement and dissemination of this report by DDC is not authorized."

(3) "U. S. Government agencies may obtain copies of this report directly from DDC. Other qualified DDC users shall request through _____."

(4) "U. S. military agencies may obtain copies of this report directly from DDC. Other qualified users shall request through _____."

(5) "All distribution of this report is controlled. Qualified DDC users shall request through _____."

If the report has been furnished to the Office of Technical Services, Department of Commerce, for sale to the public, indicate this fact and enter the price, if known.

11. SUPPLEMENTARY NOTES: Use for additional explanatory notes.

12. SPONSORING MILITARY ACTIVITY: Enter the name of the departmental project office or laboratory sponsoring *(paying for)* the research and development. Include address.

13. ABSTRACT: Enter an abstract giving a brief and factual summary of the document indicative of the report, even though it may also appear elsewhere in the body of the technical report. If additional space is required, a continuation sheet shall be attached.

It is highly desirable that the abstract of classified reports be unclassified. Each paragraph of the abstract shall end with an indication of the military security classification of the information in the paragraph, represented as *(TS)*, *(S)*, *(C)*, or *(U)*.

There is no limitation on the length of the abstract. However, the suggested length is from 150 to 225 words.

14. KEY WORDS: Key words are technically meaningful terms or short phrases that characterize a report and may be used as index entries for cataloging the report. Key words must be selected so that no security classification is required. Identifiers, such as equipment model designation, trade name, military project code name, geographic location, may be used as key words but will be followed by an indication of technical context. The assignment of links, rules, and weights is optional.